Activation of Phospholipase A_2 by Ternary Model Membranes

Adam Cohen Simonsen
MEMPHYS-Center for Biomembrane Physics, Department of Physics and Chemistry, University of Southern Denmark, Odense, Denmark

ABSTRACT Formation of liquid-ordered domains in model membranes can be linked to raft formation in cellular membranes. The lipid stoichiometry has a governing influence on domain formation and consequently, biochemical hydrolysis of specific lipids has the potential to remodel domain features. Activation of phospholipase A_2 (PLA_2) by ternary model membranes with three components (DOPC/DPPC/Cholesterol) can potentially change the domain structure by preferential hydrolysis of the phospholipids. Using fluorescence microscopy, this work investigates the changes in domain features that occur upon PLA_2 activation by such ternary membranes. Double-supported membranes are used, which have minimal interactions with the solid support. For membranes prepared in the coexistence region, PLA_2 induces a decrease of the liquid-disordered (L_d) phase and an increase of the liquid-ordered (L_o) phase. A striking observation is that activation by a uniform membrane in the L_d phase leads to nucleation and growth of L_o-like domains. This phenomenon relies on the initial presence of cholesterol and no PLA_2 activation is observed by membranes purely in the L_o phase. The observations can be rationalized by mapping partially hydrolyzed islands onto trajectories in the phase diagram. It is proposed that DPPC is protected from hydrolysis through interactions with cholesterol, and possibly the formation of condensed complexes. This leads to specific trajectories which can account for the observed trends. The results demonstrate that PLA_2 activation by ternary membrane islands may change the global lipid composition and remodel domain features while preserving the overall membrane integrity.

INTRODUCTION

Knowledge of the mechanisms that control lateral structure formation in biomembranes is crucial for understanding how membranes become organized. Domain formation in model membranes has been intensely studied in the last decade since the proposition of the raft hypothesis (1–3). Rafts are expected to be nanoscale regions of biological membranes that are linked to important cellular processes and signaling pathways (4,5).

Model membranes have provided a fundamental understanding of how phase separation and domain formation can be regulated by the lipid components (6). More specifically, the phase diagram of ternary membranes composed of cholesterol, a saturated and an unsaturated lipid, typically displays a two-phase coexistence region of the liquid-disordered L_d and liquid-ordered L_o phases. Based on a compositional analysis of biological membrane fragments (7), the liquid-ordered state in model membranes is taken to be relevant for certain aspects of rafts. Because the lipid composition controls the formation of domains, enzymatically catalyzed reactions that modify the lipid composition have the potential to induce or remodel domain features.

The interfacially activated enzyme phospholipase A_2 (PLA_2) can modulate the lipid composition of membranes by catalytic hydrolysis at the *sn*-2 position of glycerophospholipids, producing fatty acids and lysophospholipids (LysoPC) (8–10). PLA_2 activation has a significant influence on physiological functions such as inflammation (11,12). Although extensively studied by bulk assays during the past 30-plus years, the remodeling of membrane structures by PLA_2 is still poorly understood. In particular, more information is needed as to how the membrane morphology is modulated during PLA_2 activation and how this morphology is coupled to the membrane phase state (solid, liquid-disordered, liquid-ordered). PLA_2 activation has been characterized with bulk techniques such as pH-stat titration (13), (first-order) monolayer trough (14), zero-order trough measurements (15,16), and fluorescence spectroscopy (17). However, to establish a link between membrane morphology (on a nanomolar-to-micromolar scale) and PLA_2 activity, it is necessary to obtain time-resolved imaging of the hydrolysis process. This has only recently become available.

Several classes of membrane model systems are available, among which are giant unilamellar vesicles (GUVs) (18) and supported membranes. Supported membranes have inherent advantages in the characterization techniques that can be applied and the planar geometry facilitates image interpretation and analysis. Single-supported membranes prepared by vesicle fusion or Langmuir-Blodgett deposition are widely used, but are prone to unwanted interactions with the support surface that can alter membrane properties compared to a freestanding membrane (19,20). These issues are largely overcome by utilizing a double-supported (distal) membrane which is separated from the solid support by a lower (proximal) membrane. We have recently developed a procedure to prepare single- and double-supported bilayers based on the hydration of spin-coated lipid films (21). We have found this method to be applicable to all membrane compositions tested and to be robust toward the presence of salt in the aqueous phase. Full coverage of the proximal bilayer is easily

Submitted June 20, 2007, and accepted for publication December 31, 2007.

Address reprint requests to Adam Cohen Simonsen, E-mail: adam@memphys.sdu.dk.

Editor: Petra Schwille.

0006-3495/08/05/3966/10 $2.00

doi: 10.1529/biophysj.107.114363

obtained by appropriate adjustment of the lipid concentration in the coating solution. Patches or extended regions of double bilayers are easily prepared (22). We recently demonstrated (23) that double-supported ternary membranes can display circular domain morphologies which are highly similar to the ones observed in GUVs.

In the last decade, direct imaging by atomic force microscopy (AFM) of supported membranes subjected to enzymatic hydrolysis has been reported in a number of studies. Most PLA_2 studies have been done with membranes in the solid-ordered phase such as DPPC (24–27) and facilitated by the mechanical stability of solid membranes. Some studies have also reported on the activation of triacylglycerol lipases by mixed supported bilayers of DPPC and glycerolipids (28,29). However, membranes in the fluid state are much more relevant as biological model systems, but their increased lateral lipid mobility makes them more difficult to study over extended times using AFM. Based on recent advances in sample preparation methodology (21) we have demonstrated by fluorescence microscopy (30) that PLA_2 activation by a fluid-supported membrane can result in complex restructuring of the membrane morphology during hydrolysis. This behavior is not seen in solid membranes and is attributed to the combined effect of line tension and membrane fluidity. Although addressed by bulk assays (31,32), very few studies have visualized the enzymatic remodeling of membranes with a particular lipid-controlled lateral structure such as domains (33). One example is the activation of PLA_2 by double-supported membranes in the ripple phase (34). This study demonstrated changes in the ripple spacing and eventual disappearance of the ripples, suggesting that PLA_2 induces lipid compositional changes while maintaining membrane integrity. Recently, two separate AFM studies of ternary membranes, i.e., DOPC, sphingomyelin, and cholesterol, exposed to sphingomyelinase, demonstrated how in situ generation of ceramide leads to formation of elevated subdomains (35,36).

This article reports on PLA_2 activation by ternary model membranes composed of two phospholipids (DOPC, DPPC) and cholesterol. Time-lapse fluorescence imaging documents the effect of PLA_2 on preexisting domains and demonstrates a phenomenon by which an initially homogenous membrane, prepared outside the two-phase region, develops liquid domains during the hydrolytic activity. By image analysis, the evolution in membrane domain areas is followed during hydrolysis.

MATERIALS AND METHODS

Materials

1,2-dioleoyl-*sn*-glycero-3-phosphocholine (DOPC), 1,2-dipalmitoyl-*sn*-glycero-3-phosphocholine (DPPC), cholesterol (Chol), 1-oleoyl-2-hydroxy-*sn*-glycero-3-phosphocholine (Oleoyl-LysoPC), and 1-palmitoyl-2-hydroxy-*sn*-glycero-3-phosphocholine (Palmitoyl-LysoPC), were obtained from Avanti Polar Lipids (Alabaster, AL). Palmitic acid, oleic acid, and other chemicals were from Sigma (St. Louis, MO). 1,1′-Dioctadecyl-3,3,3′,3′-tetramethylindocarbocyanine perchlorate ($DiIC_{18}$) was obtained from Invitrogen (Carlsbad, CA). Wild-type porcine pancreatic phospholipase A_2 was a gift from Novozymes (Bagsværd, Denmark).

Ultrapure Milli-Q water (18.3 MΩ·cm; Millipore, Billerica, MA) was used in all steps involving water. HEPES buffer (10 mM HEPES, 150 mM NaCl, 30 μM $CaCl_2$, and 10 μM EDTA) was prepared at pH = 7.5 by mixing appropriate amounts of HEPES and HEPES sodium salt. Muscovite mica (75 mm × 25 mm × 200 μm sheets) was from Plano (Wetzlar, Germany). Mica sheets of 10 mm × 10 mm were glued onto round (0.17 mm, Ø24 mm) microscope coverslips using a transparent and biocompatible silicone glue (catalog No. MED-6215; Nusil Technology, Santa Barbara, CA). Immediately before use, the mica was cleaved with a knife leaving a thin and highly transparent mica film on the coverslip.

Preparation of double-membrane islands

The preparation of fluid membrane islands is an extension of the methodology we recently developed (21) for preparing single-supported membranes by hydration of spin-coated lipid films. This procedure is somewhat different from conventional protocols in that the formation of dehydrated, stacked bilayers by self-assembly takes place during the spin-coating step. The subsequent hydration and annealing serves to equilibrate the membrane in an aqueous environment and to release excess bilayers into solution.

This version of the method consists of two steps: 1), fabrication of a dry spin-coated lipid film, followed by 2), controlled hydration/annealing of the film.

To prepare a dry spin-coated lipid film on mica we used a stock solution of 10 mM total lipid containing 0.7% DiI-C_{18} in a hexane/methanol (97:3 volume ratio). A droplet (30 μl) of this lipid stock solution was then applied to freshly cleaved mica with a size 10 mm × 10 mm and immediately thereafter spun on a model No. KW-4A spin-coater (Chemat Technology, Northridge, CA) at 3000 rpm for 40 s. This created a dry multilayered lipid film which was then placed under vacuum in a desiccator for 10–15 h to ensure complete evaporation of solvents. The dry spin-coated film was subsequently hydrated by immersing the sample in HEPES buffer followed by heating in an oven to 80°C for 1 h.

The sample was then placed on the fluorescence microscope (see below) and flushed with 80°C buffer. By monitoring the response of the lipid film with 4× magnification, the removal of lipid layers could be accurately controlled. Typically, only the center of the sample was flushed and this completely removed all but the lowest bilayer in this region. Some distance away from the flushed region, lipid multilayers where present, while in the transition zone one could routinely localize round double bilayer islands situated on top of the lowest bilayer. Once such a region with round bilayer islands had been localized, the sample was allowed to cool to 20°C and to relax for at least 1 h before the addition of PLA_2.

Fluorescence microscopy

Epi-fluorescence microscopy of the lipid film was performed with the sample placed with the lipid side facing up in a custom-made microscope chamber (2 ml volume) and placed on a model No. TE2000 inverted microscope (Nikon, Melville, NY) and using an oil immersion objective (Plan Apo, 60×, NA = 1.4; Nikon). Fluorescence excitation was done with a halogen lamp and using a G-2A filtercube (Nikon). Images were recorded with a high sensitivity CCD camera (SensiCam EM, 1004 × 1002 pixels; Cooke, PCO-Imaging, Kelheim, Germany) and operated with Camware software (PCO-Imaging). Lipid hydrolysis was initiated by completely exchanging the HEPES buffer in the microscope chamber with a HEPES buffer containing PLA_2 without drying or moving the sample. Images were recorded at 10 s intervals. A total of 300–500 images where recorded before experiment. All experiments were conducted at room temperature (20°C).

Image analysis

Image analysis of the fluorescence time series was automated with custom m-files written in MATLAB (The MathWorks, Natick, MA). Segmentation of the island to detect the total island area as well as the areas of the liquid-ordered and liquid-disordered phases was done by conversion to binary images by a cutoff approach. Two different cutoff values were employed with the purpose of 1), separating the island outer contour from the underlying membrane; and 2), separating the L_o and L_d phases within the membrane island. Segmentation by this approach is possible if the distribution of the lipid dye among the two membrane phases is different in the proximal and the distal membranes. To be more specific, consider the following reasoning: Let H and L denote the fluorescence intensity of the L_d and L_o phases in the membrane island and let h and l denote the corresponding intensities in the underlying membrane. Segmentation according to the criteria 1 and 2 mentioned above is possible, given the inequalities

$$L > h - l \tag{1}$$

and

$$H - L > h - l. \tag{2}$$

This is, for example, satisfied for the values $(H,L) = (0.7,0.3)$ and $(h,l) = (0.6,0.4)$. That such intensity differences do exist is confirmed by direct evaluation of the pixel intensities in the measured images (not shown). One possible explanation for the different partitioning of the dye in the upper and lower bilayers can be that the probe (DiI-C_{18}) is positively charged and therefore attracted to the negative mica. This attraction may influence the partitioning of the dye among the membrane phases and will be larger for the proximal than for the distal bilayer. Note that the cutoff values were gradually decreased with time to compensate for slight photobleaching during the time-series. By color-coding the two resulting images, the segmented islands could be visualized as shown in Fig. 4 (*inset*).

RESULTS

PLA_2 activation by a ternary membrane prepared in the coexistence region

The specific membrane model system used in this work consists of secondary membrane islands separated from the mica substrate by a primary membrane adjoining the support (Fig. 1 *A*). Due to its flatness, mica is normally the substrate of choice for atomic force microscopy (AFM) on supported membranes, but we have found that mica also provides an ideal and uniform substrate for fluorescence studies of supported membranes. Although glass has superior optical properties compared to mica, its micro-roughness can interfere with the formation of lateral membrane structures. For this reason, fluid membrane islands typically do not appear round on a glass substrate due to pinning of the membrane edges by glass protrusions. The substrate indicated in Fig. 1 *A* consists of a mica sandwiched with a glass coverslip using a transparent and biocompatible silicone elastomer. This system takes advantage of the flatness of mica as substrate, but at the same time provides optimum optical transparency by allowing the mica to be cleaved to an ultrathin film which is mechanically supported by the glass. The total thickness of the substrate sandwich can be kept below the working distance (210 μm) of our high NA oil-immersion objective.

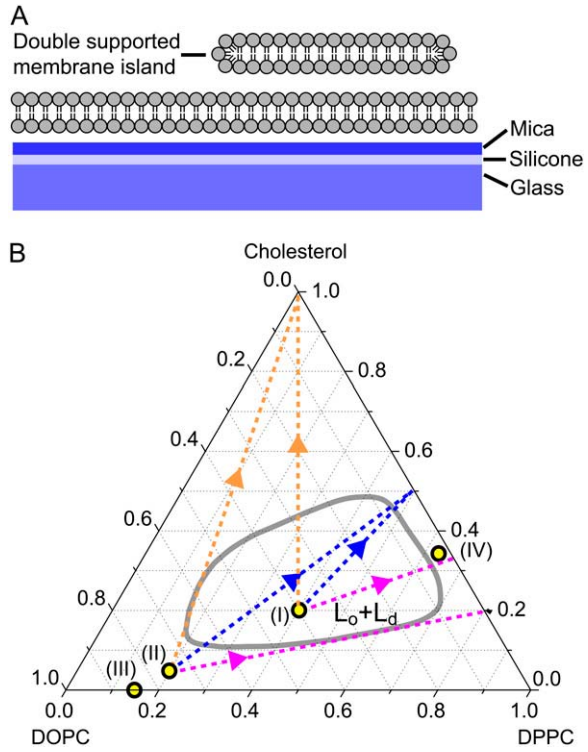

FIGURE 1 Configuration of the double-supported membrane model system used in this work (*A*). Phase diagram (*B*) at 20°C for a ternary membrane (DOPC/DPPC/cholesterol) where the liquid-ordered/liquid-disordered (L_o + L_d, *red line*) coexistence region was adapted from Veatch and Keller (37). The yellow markers (*I–IV*) denote the compositions used in Figs. 2–6. The dotted lines indicate possible compositional alterations to (*I*) and (*II*) assuming removal of DOPC only (*purple*), assuming approach toward a 1:1 ratio of DPPC to cholesterol (*blue*) or assuming removal of DPPC and DOPC with equal probability (*orange*).

Double-supported membranes are known from several studies to display domain patterns which are in very good agreement with the structures found in the corresponding freestanding membranes (23). We have previously demonstrated (22) that double-supported membranes can be used as an appropriate model system to investigate PLA_2 activity by time-lapse recording of fluorescence images during the lipid degradation. In this process, the membrane islands maintain a uniform round shape which is easily detected by image analysis algorithms. By invoking a simple kinetic model it is possible to extract parameters from the image data describing enzyme turnover and enzyme-membrane binding constants. This analysis suggested that PLA_2 mainly attacks the membrane island at the exposed edges while little or no activation occurs on the membrane surface. This work can be viewed as a continuation of these studies to investigate the PLA_2 activation by domain-forming ternary membranes.

Fig. 1 *B* shows the phase diagram of DOPC/DPPC/Cholesterol membranes determined by fluorescence microscopy of GUVs. The phase diagram is only partially known, but much attention has been dedicated by Keller et al. (37) in mapping the boundary of the two-phase region (*red line*).

More complete phase diagrams have recently been published (see (52,53)). Membranes prepared inside this coexistence region display phase separation into two fluid domains we denote liquid-ordered (L_o) and liquid-disordered (L_d) phases. The precise composition of the membrane domains is given by drawing a tieline from the membrane composition to the boundary of the coexistence region. The approximate direction of the tielines goes from the DOPC vertex to the 1:1 point of the DPPC, cholesterol edge (38,39). Consequently, the L_o phase is enriched in DPPC and cholesterol while the L_d phase is enriched in DOPC. The lipid dye (DiI-C_{18}) used in this study partitions preferentially into the L_d domains such that L_o domains appear dark in the fluorescence images. Both phospholipids (DOPC,DPPC) used in this study are potential substrates for PLA_2 if presented to the enzyme in a conformation which matches the active site.

Fig. 2 *A* shows an example of a membrane island with the composition (*I*) as indicated in Fig. 1 *B*. Both the upper and the lower membranes display domain formation and therefore overlapping domain features are observed in the region of the island. Domains in the island are generally larger than in the lower membrane due to interaction of this membrane with the support, limiting the lateral lipid mobility (23). The fluid nature of the domains is evident from their rounded shapes. Both domain types are exposed at the edge of the island where PLA_2 activation will occur.

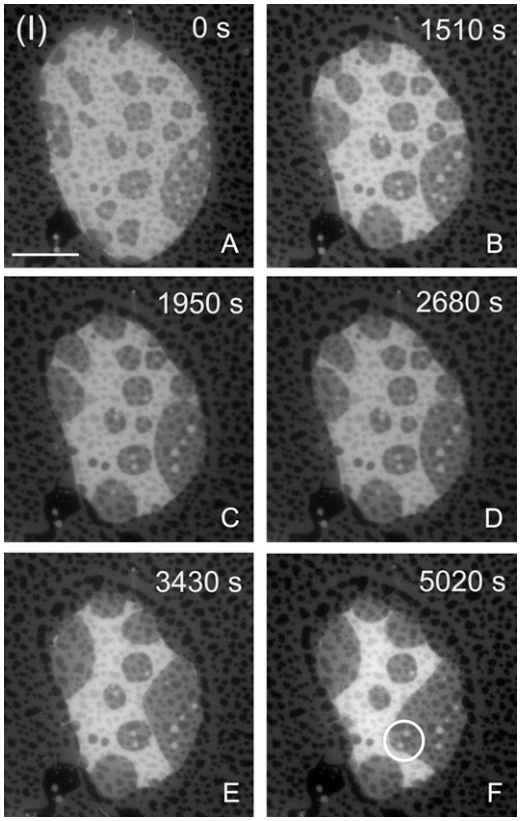

FIGURE 2 Temporal evolution (*A–F*) of a membrane island with the initial composition (*I*) in Fig. 1 and after addition of PLA_2 (200 nM) at time $t = 0$ s. The area of the liquid-disordered (*bright*) phase decreases relative to the liquid-ordered (*dark*) phase. Overlapping domains in both the proximal and distal membranes are apparent. (Scale bar: 20 μm.)

Upon addition of PLA_2 to the fluid cell at time $t = 0$ s, hydrolysis proceeds immediately as observed by a gradual decrease in the area of the island (Fig. 2, *A–F*). No lag phase is observed, in agreement with our previous observations of pure POPC membrane islands. The absence of a lag phase can be attributed to the exposure of the free membrane edge at the island boundary, which provides suitable defect sites for the enzyme to attack immediately. During hydrolysis, two distinct features are observed. One is the coalescence of domains and the formation of larger domain structures. This coarsening dynamics is inherent to a membrane that is cooled into the coexistence region (23), but appears accelerated by the activity of PLA_2. The other distinct feature is the decrease in the relative area of the bright L_d phase as compared to the dark L_o phase. If allowed to proceed for extended times, the bright phase eventually disappears while the dark phase remains static. However, as seen in Fig. 2 *F*, the fraction of the total island edge which presents the bright phase to the enzyme decreases during hydrolysis and eventually only thin domain stripes extent to the edge. This will limit the accessibility of PLA_2 to the bright phase and slow down the reaction. A striking example of this is found in the small bright domain inclusions inside the dark phase (*bright circle* in Fig. 2 *F*). These domain inclusions resist hydrolysis over the entire interval shown in Fig. 2, *A–F*, probably because they are not connected to the island edge and therefore not readily accessible to the enzyme.

To examine the properties of each of the two domain types in Fig. 2, several islands each consisting of one single homogenous phase were now prepared outside the coexistence region and exposed to PLA_2.

PLA_2 activation by an L_d-membrane prepared outside the coexistence region: domain formation

The results presented in Fig. 2, *A–F*, demonstrates substantial changes to the domain pattern and the domain areas after exposure of the membrane to PLA_2. To understand this behavior in more detail it is relevant to examine the response of membranes consisting of uniform L_d and L_o phases.

Fig. 3 *A* shows a membrane island with the composition (*II*) marked in the phase diagram of Fig. 1 *B* and corresponding to DOPC/DPPC/Cholesterol of (75:20:5). This point falls just outside the (L_o,L_d) coexistence region and based on generic tielines calculated by Radhakrishnan and McConnell (39), which approximates the composition of the bright L_d phase in composition (*I*) (Fig. 2 *A*). When the membrane island with composition (*II*) in Fig. 3 *A* is subjected to hydrolysis by addition of PLA_2, a gradual decrease in membrane area is initially observed. After a decrease in membrane area by ~30%, dark domain features starts to

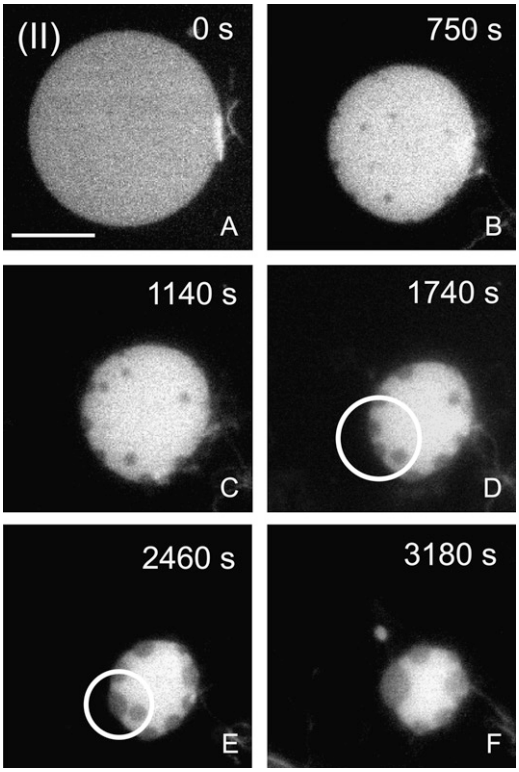

FIGURE 3 Evolution of a membrane island with the initial composition (*II*) in Fig. 1 after PLA_2 injection at time $t = 0$ s. During hydrolysis, condensed liquid-ordered-like domains (*dark*) emerge from the initially homogenous liquid-disordered phase. Domain coalescence of these domains as indicated by the circles in panels *D* and *E* demonstrate the membrane fluidity. (Scale bar: 20 μm.)

nucleate in the island (Fig. 3 *B*). The total area of these dark domains is increasing while the total membrane area continues to decrease (Fig. 3, *B–F*). The emerging dark domains are clearly in a fluid state, as seen by the rounded shapes of these domains and the fact that dark domains coalesce into larger domains that are also round. An example of domain coalescence is shown in the marked region (*circles*) of Fig. 3, *D* and *E*. Lateral diffusion of dark domains in the bright matrix is observed, such as in images taken around the time of Fig. 3 *C*. However, when dark domains contact the island edge they are permanently immobilized at the edge and take on a distorted lenslike shape. This behavior suggests a two-dimensional wetting phenomenon where L_o domains are occupying the island edge. This is likely to be driven by a smaller line tension of the L_o compared to L_d domain, which makes it energetically favorable for the system to distribute the L_o phase at the island edge.

The domain formation observed in Fig. 3 is quite intriguing and implies that the compositional changes to the membrane caused by PLA_2 activity are sufficiently large to induce domain formation. The dark domains in Fig. 3 have a striking similarity to the liquid-ordered domains observed for a membrane prepared in the coexistence region (Fig. 2 *A*). The PLA_2-induced domains are excluding the fluorescent probe, which also suggests that the lipid packing properties are similar to the L_o phase. For these reasons, we will refer to the PLA_2-induced domains in Fig. 3, *B–F*, as liquid-ordered.

Quantification of domain areas

There are several common features between the results obtained in Figs. 2 and 3. In both cases, the activity of PLA_2 leads to changes in the ratio between L_o and L_d domains such that the area ratio A_{L_o}/A_{L_d} increases during PLA_2 activity. These common features can be examined further if the domain areas and the total membrane area are quantified. This has been done in Fig. 4, which shows a quantitative analysis of the image data in Figs. 2 and 3 corresponding to the initial compositions (*I*) and (*II*). The plots show the absolute areas of the L_o and L_d phases within an island as well as the total island area.

While the total membrane area is decreasing monotonically in both Fig. 4, *A* and *B*, this decrease is the sum of opposite changes in the area of L_o and the L_d phases. In fact, the area of the L_d phase is decreasing in both cases while the area of the L_o phase is either zero or increasing. For the island in Fig. 2, it is somewhat surprising that the area of the dark L_o phase is increasing, since this fact is not obvious from a visual inspection of the images. It clearly demonstrates that hydrolysis does not simply lead to removal of material from the L_d phase, but also modifies the global lipid composition and thereby leads to an increase of the L_o phase.

A common property of the curves in Fig. 4, *A* and *B*, is that both systems go through a crossover point were the majority phase changes from being the L_d to becoming the L_o phase while the overall area decreases. However, an important difference is that the dynamics in Fig. 4 *A* is significantly slower than in Fig. 4 *B* because the island in the first case is larger and therefore has a smaller perimeter/area ratio. Since PLA_2 activation occurs preferentially at the membrane edge, the rate of area change dA/dt scales with the perimeter length L (22).

Control experiments

Formation of the liquid-ordered phase in membranes requires the presence of cholesterol (40) which induces a chain ordering of saturated phospho- or sphingolipids such as DPPC. The PLA_2-induced appearance of a liquid-ordered-like phase in Fig. 3 therefore suggests that the cholesterol content of this system might play a critical role in the domain formation observed during hydrolysis. To test this hypothesis, another membrane composition without cholesterol was chosen. This is marked (*III*) in Fig. 1 *B* and is a binary mixture of DOPC,DPPC in the ratio (85:15). This composition is quite close to the point (*II*) in the ternary phase diagram, but with the difference that cholesterol is absent.

The thermal phase diagram of the DOPC/DPPC system displays a broad solid/liquid-disordered coexistence region,

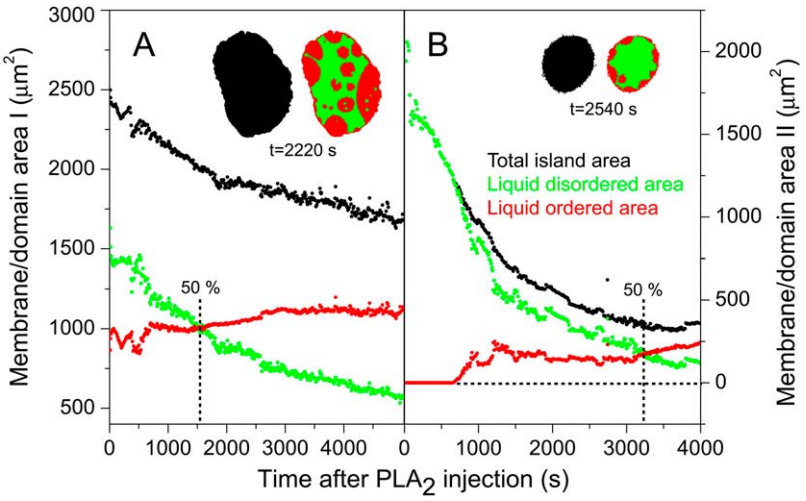

FIGURE 4 Time-resolved quantification of the total island area as well as areas of the L_o and L_d domains after injection of PLA_2 (200 nM) at $t = 0$ s. Curves in panels *A* and *B* are constructed from the image data in Figs. 2 and 3, respectively. Black points denote the total area A_{tot} of the membrane island while green and red points are the areas of the liquid-disordered A_{L_d} and liquid-ordered A_{L_o} phases within the island. Areas always satisfy the relation $A_{tot} = A_{L_d} + A_{L_o}$. The inserts show examples of the segmentation of an island into domains. As indicated, data in both panels *A* and *B* go through a crossover point corresponding to equal areas of the two domain types.

as calculated by Elliott et al. (41). At 20°C the composition (*III*) falls outside this coexistence region corresponding to the membrane being in a uniform L_d state. Fig. 5 *A* shows a membrane island prepared with the composition (*III*). Upon hydrolysis of this membrane island by PLA_2, a gradual decrease in membrane area is observed, but without the formation of domains. No domains are formed, not even after a >50% decrease in the total membrane area (Fig. 5 *C*). This is a clear result which demonstrates that when cholesterol is removed, the domains observed in Fig. 2 are no longer appearing. It supports the notion that the PLA_2-induced domains are in a liquid-ordered state since Fig. 5, *A–C*, demonstrates that cholesterol is required for their formation.

The increase in the area of the liquid-ordered phase as observed in the curves of Fig. 4 indicates that the phospholipid component of this phase is resistant to hydrolysis. This resistance against PLA_2 activation was confirmed by another control experiment in which a homogenous membrane island in the L_o state was prepared. Fig. 5 *D* shows such a membrane island with composition (*IV*) = 62:35:3 in Fig. 1 *B*. Based on the phase diagram in Fig. 1 *B*, this composition corresponds to a uniform L_o membrane. When this membrane is subjected to PLA_2 for prolonged times, no area change can be observed suggesting that PLA_2 is not activated by this membrane (Fig. 5, *D–F*). This result points to a critical role of cholesterol in regulating PLA_2 activation and suggests that cholesterol is able to partially or completely block the activation of PLA_2 by DPPC.

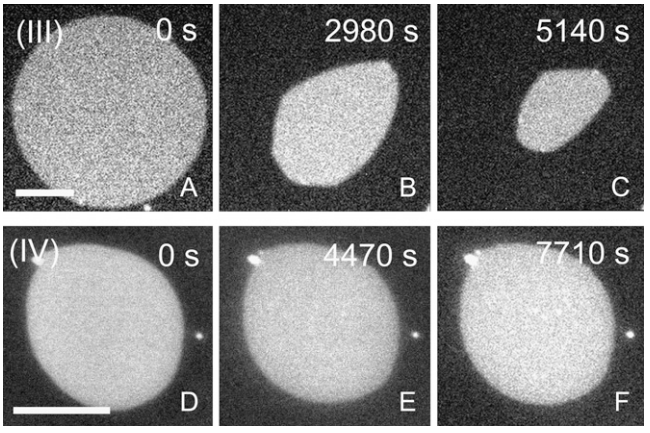

FIGURE 5 Control experiment testing the influence of PLA_2 on membrane islands with initial compositions (*III*) and (*IV*) marked in Fig. 1 and with the time after PLA_2 injection as indicated. The fluid binary membrane (composition (*III*)) displays area decrease without domain formation at any time of the reaction (*A–C*). Conversely, the initial composition (*IV*) corresponding to the liquid-ordered phase is resistant to hydrolysis and exhibits no detectable area change. (Scale bar: 20 μm.)

Another issue concerns the possible role of the reaction products (Lyso-PC and fatty acids) in modifying the membrane domain morphology. Hydrolysis of both phospholipids in a ternary membrane with composition DOPC/DPPC/Chol yields two reaction products per phospholipid such that a partially degraded membrane may in principle have seven components. The extent to which these reaction products partition into the remaining bilayer or are carried into solution is not known with certainty. This important issue determines whether a partially degraded membrane island can be mapped onto a ternary phase diagram or not. A successful correlation of initial reaction rates with the phase diagram of binary mixtures (42) have demonstrated that this is potentially a powerful approach for rationalizing PLA_2 activation.

First of all it should be noted that a decrease in the total membrane area as observed in the islands of Figs. 2 and 3 is evidence that a net removal of material takes place during reaction. Our previous study (22) of PLA_2 activation by one-component POPC membrane islands has given some further insight into the possible accumulation of reaction products. In this study, the decrease in membrane area was used as input to a simple kinetic model which gave an estimate of turnover numbers as well as PLA_2-membrane binding constants. Turnover numbers compared favorably with literature values determined by bulk assay, indicating that the area decrease could be quantitatively linked to a known

enzyme activity. In this study, a control experiment using β-cyclodextrin (βCD) was carried out to ensure removal of reaction products by complexation to βCD. The result showed that the measured turnover numbers were unaffected by addition βCD, thus confirming that the reaction products did not have a significant influence on the measured areas. However, the PLA_2-membrane affinity decreased upon βCD addition, which indicates that removal of the negatively charged reaction products lowers the attraction of PLA_2 to the membrane. Thus, low-level accumulation of reaction products around the site of the enzyme cannot be ruled out. However, this accumulation is not large enough to affect the total membrane area, and is therefore not likely to significantly influence the global lipid composition.

In this study it not possible to make a similar control experiment with βCD because this would also remove cholesterol from the membrane. Alternatively, we study the impact of the reaction products by attempting to prepare membranes containing these components. Fig. 6 *A* shows a single-supported ternary membrane with the composition I inside the (L_o,L_d)-coexistence region. This membrane exhibits domain formation. Control samples were now prepared where each of the phospholipids in this system were replaced with the corresponding reaction products. Thus Fig. 6 *B* shows membrane in which DPPC is replaced with its reaction products (Palmitic acid and Palmitoyl-LysoPC) and in Fig. 6 *C* DOPC is replaced with Oleic Acid and Oleoyl-LysoPC. These membranes containing the reaction products were prepared by spin-coating, as described in Materials and Methods. The resulting membranes could only be made to cover the support surface in patches and double membranes could not be prepared. These observations testify to the membrane destabilization induced by the reaction products. In the images of Fig. 6, *B* and *C*, domains are absent. The absence of nanoscale domains was confirmed by separate AFM imaging of these membranes (not shown). It is likely that the membranes in Fig. 6, *B* and *C*, do not contain the same proportion of products as in the coating solution. If this is the case, it means that such high concentrations of products are also unlikely to be present in the membrane islands. Therefore this control shows that, when attempting to incorporate reaction products at high concentrations, the resulting membranes are domain-free in contrast to the original ternary membranes without reaction products.

Correlation with phase diagram trajectories

Taken together, the results described above indicate that reaction products may possibly be present locally in the membrane where PLA_2 is active, but at levels which do not significantly influence the global membrane composition. Moreover, reaction products are unlikely to be responsible for the PLA_2-induced domain formation in Fig. 3, and it should therefore be explained by a different mechanism. Based on these considerations, it is appropriate to attempt an interpretation of the results in Figs. 2 and 3 using the hypothesis that partially degraded membrane islands can be mapped onto the ternary phase diagram in Fig. 1 *B*. The typical lipid lateral diffusion constant D_L for fluid membranes with cholesterol is $\sim 10 \times 10^{-12}$ m^2/s (43). This gives an average two-dimensional displacement over the time interval between image frames ($t = 10$ s) of $\langle r_{2D} \rangle = \sqrt{4D_L t} = 20\mu m$. Comparing with the island size in Figs. 2 and 3, $\langle r_{2D} \rangle$ is so large that the islands are unlikely to develop a lateral compositional heterogeneity and therefore an equilibrium description of the entire island is justified.

There are several possible schemes for the changes in the membrane composition during hydrolysis depending on differences in the relative removal of DPPC and DOPC (*dashed lines* in Fig. 1 *B*). Considering the island with composition (*II*) in Fig. 3 *A*, we can disregard a selective removal of DPPC since this would move the composition in the opposite direction of the coexistence region. Another possibility is selective removal of DOPC, which shifts the composition on a line (*purple*) touching the border of the coexistence region. Removal of DOPC and DPPC with equal probability creates another line (*orange*) also at the border of the coexistence region. None of these options can account for the observed trends in Fig. 3.

A last option is that the membrane approaches a specific stoichiometric ratio of DPPC/Cholesterol, for example (1:1). This gives rise to a line (*blue*) running across the coexistence region which would imply formation of (L_o,L_d) domains during hydrolysis. This model is motivated by the proposition of Radhakrishnan and McConnell (39,44,45) that so-called condensed complexes in ternary membranes may form between cholesterol and the saturated lipid component (DPPC). The average stoichiometry of the complexes is typically taken as 1:1. An obvious possibility is now that DPPC, when part of such condensed complexes, is inaccessible to PLA_2

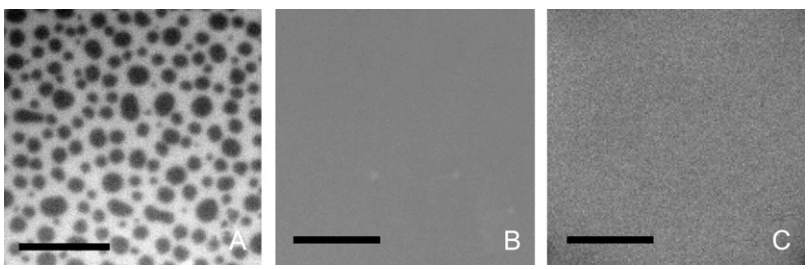

FIGURE 6 Control experiment demonstrating absence of domains in membranes containing the reaction products. Domains in a single-supported membrane with composition (*I*) are shown (*A*). When the DPPC of the membrane (composition (*I*)) is replaced by its hydrolysis products (Palmitic acid and Palmitoyl-LysoPC), membrane domains are absent (*B*). The same absence of domains is observed (*C*) when DOPC of the membrane (composition (*I*)) is replaced with the corresponding hydrolysis products (Oleic Acid and Oleoyl-LysoPC). (Scale bar: 10 μm.)

and therefore resists hydrolysis. This may happen even if the complex formation does not lead to large-scale phase separation. Assuming now that phospholipids which are not associated with cholesterol are removed with an equal probability, this creates the blue line in Fig. 1 *B*. In this scenario the point 1:1 (DPPC/Cholesterol) becomes an attractor that the membrane composition approaches during hydrolysis.

Fig. 7 plots the ratio of L_o to L_d domain area versus the total island area. The total island area has been normalized to the value where the L_o and L_d phases have equal areas such that all data sets traverse the point (1,1). The figure shows simulated data (*solid line*) corresponding to the blue trajectory in Fig. 1 *B* and also indicated in the insert of Fig. 7. For simplifying the calculation of the L_o/L_d ratio, it was assumed that this trajectory coincides with a tieline, in agreement with theoretical predictions (39). Fig. 7 also includes the data for islands (*I*) and (*II*). For increasing time (decreasing total area), the simulation shows nucleation of the liquid-ordered domains at ~45% of the initial membrane area. There is an overall excellent agreement between the simulated trajectory and the data for islands (*I*) and (*II*), but with the data for island (II) showing a slightly faster initial increase in the L_o area. The simulation also accounts for the evolution in domains areas of island (*I*). Thus, Fig. 7 demonstrates that, to a first approximation, a quantitative correlation can be made between the measured evolution in L_o,L_d domain areas and a simulated trajectory in the ternary phase diagram. The trajectory approaches a 1:1 stoichiometric ratio of DPPC/cholesterol. But given the uncertainties in the phase diagram and the tielines, the current analysis cannot discriminate between trajectories with a slightly different stoichiometry than 1:1. However, the analysis in Fig. 7 clearly indicates that the notion of resistant condensed complexes provides a better description of the measured trends than the alternative options described by the purple and orange tracks in Fig. 1 *B*.

It is useful to reconsider the behavior of the membrane with initial composition (*III*) in Fig. 5, *A–C*, and attempt an interpretation of this result in terms of the binary DOPC, DPPC phase diagram. This membrane did not develop domains during hydrolysis, indicating that DOPC and DPPC were removed with equal probability. If DOPC had been preferentially removed, the composition would eventually have shifted into the adjoining solid-fluid coexistence region of the DOPC/DPPC phase diagram (41) and solid domains would have emerged. The fact that domains remain absent upon hydrolysis of composition (*III*) while domains are forming in composition (*II*) clearly points to a critical role of cholesterol in protecting DPPC against hydrolysis by PLA_2.

It is well established that cholesterol induces acyl-chain ordering and has a lateral condensing effect on DPPC membranes above the main melting point. Molecular dynamics simulations by Smondyrev and Berkowitz (46) have provided further atomistic insight into the molecular conformations of mixed DPPC/cholesterol membranes. Interestingly, this study demonstrated that there is a strong tendency of the *sn*-2 carbonyl oxygen of DPPC to form hydrogen bonds with the carboxyl group of cholesterol. Moreover, recent experiments and simulations by Peters and co-workers (47,48) have shown that chemical modifications to natural lipid substrates will influence PLA_2 activity by modifying water access to the active site. The simulations also revealed that Ca^{2+} stabilizes the lipid substrate by coordination to the *sn*-2 carbonyl oxygen. It is possible that cholesterol may compete with Ca^{2+} in coordinating to the DPPC *sn*-2 carbonyl oxygen atom. At the same time access of water to the active site may also be influenced by cholesterol.

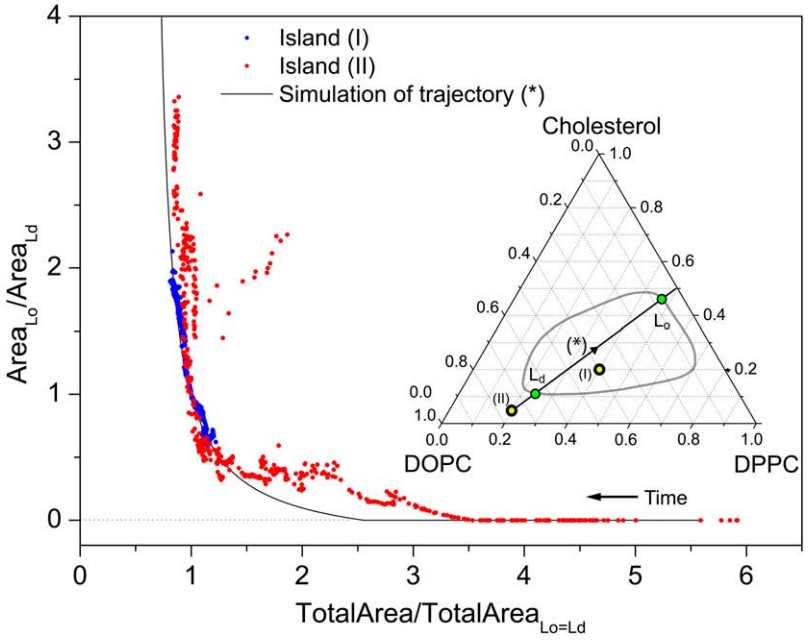

FIGURE 7 Plot of the ratio of L_o/L_d domain area versus the total island area. The total island area is normalized to the value where the L_o and L_d phases are equally large. This normalization enables a comparison of data for islands (*I*) and (*II*) displayed in Fig. 4. Black line is data for a simulated trajectory across the L_o/L_d-coexistence region as shown in the insert. For the simulated trajectory it is assumed that the trajectory is also a tieline such that the composition of the domains is given by the intercepts with the phase boundaries (*green circles*). Blue and red points are data from islands (*I*) and (*II*) of Fig. 4, respectively.

It therefore appears likely that formation of DPPC/cholesterol complexes may interfere with the delicate steric conditions in the active site that are necessary for hydrolysis to occur. This, in turn, might explain why PLA_2 is not activated by DPPC membranes in the L_o phase.

Biomembranes are structurally and compositionally much more complex than binary and ternary model systems and a straightforward correlation is not possible. However, cholesterol has been shown to be a key lipid for the formation of fluid domains in biomembranes such as pulmonary surfactants (49). It is likely that cholesterol will also be an important regulator of PLA_2 activation in biomembranes and facilitate protection of certain substrate species by formation of condensed complexes or liquid-ordered-like membrane phases. It should also be mentioned that PLA_2 has been linked to atherosclerosis (50). Thus, overexpression of human PLA_2 (type IIa) in mice correlates with elevated atherosclerotic lesions (51). In this context, this study points to a mechanism whereby membranes with elevated cholesterol content can be generated by PLA_2 activation.

CONCLUSION

This work has demonstrated that PLA_2 is capable of inducing substantial changes in the domain morphology of ternary membranes containing two phospholipids and cholesterol. For a membrane with an initial composition (*I*) within the (L_o,L_d) coexistence region, PLA_2 activation leads to a decrease in the L_d phase, an increase in the L_o phase, and an overall area decrease. A membrane prepared in the L_d phase (*II*) outside the coexistence region develops L_o-like domains during hydrolysis. Both membranes with initial compositions (*I*) and (*II*) pass through a 50% crossover point where the majority phase shifts from the L_d to the L_o phase.

Control experiments confirm that this behavior is tightly coupled to cholesterol which, although not itself hydrolyzed by PLA_2, appears as a key lipid for regulating PLA_2 activation and the resulting membrane domain pattern. An important clue is that PLA_2 is not activated by a membrane in the L_o phase. An attempt is made to rationalize the observed trends using the hypothesis that the ternary phase diagram can be used to map partially hydrolyzed membrane islands. In this picture, specific trajectories in the ternary phase diagram are constructed describing the compositional changes. The possible accumulation of reaction products was investigated previously (22) and these results lend support to the validity of this approach. The results are in accordance with the formation of condensed cholesterol/DPPC complexes in which DPPC resists hydrolysis through its affinity to cholesterol. During hydrolysis the membrane will then approach a PLA_2-resistant stoichiometric ratio between DPPC and cholesterol. Such trajectories can account for the current experimental observations.

The results underline that PLA_2-catalyzed hydrolysis of a phase-separated fluid membrane does not simply imply static removal of material from one phase. Rather, the global lipid composition is altered according to a specific underlying principle in which cholesterol is a key player. The trajectories toward one common attractor point in the phase diagram comprise a visual representation of this principle. The changes in the global lipid composition will impact the membrane domain morphology, depending on how the trajectories are localized with respect to coexistence regions of the phase diagram.

This study has demonstrated the usefulness of membrane islands as a novel biophysical membrane model system. The double-supported membrane design virtually eliminates previous problems of supported membranes related to interactions with the solid support. The size of the membrane islands used in this study corresponds well to typical cell-sizes as well as to the typical size of GUVs used for confocal microscopy. In contrast to spherical membranes, the planar geometry of the membrane islands facilitates image analysis and quantification of the membrane and domain areas.

I thank Chad Leidy and Ole G. Mouritsen (MEMPHYS) for helpful discussions.

I thank The Danish National Research Foundation for support via a grant to MEMPHYS-Center for Biomembrane Physics; The Augustinus Foundation; and The European Commission under contract No. NMP4-CT-2003-505211 (BIOSCOPE).

REFERENCES

1. Simons, K., and E. Ikonen. 1997. Functional rafts in cell membranes. *Nature*. 387:569–572.
2. Edidin, M. 2003. The state of lipid rafts: from model membranes to cells. *Annu. Rev. Biophys. Biomol. Struct.* 32:257–283.
3. London, E. 2005. How principles of domain formation in model membranes may explain ambiguities concerning lipid raft formation in cells. *Biochim. Biophys. Acta*. 1746:203–220.
4. Jacobson, K., O. Mouritsen, and R. G. W. Anderson. 2007. Lipid rafts: at a crossroad between cell biology and physics. *Nat. Cell Biol.* 9:7–14.
5. Mayor, S., and M. Rao. 2004. Rafts: scale-dependent, active lipid organization at the cell surface. *Traffic*. 5:231–240.
6. Veatch, S. L., and S. L. Keller. 2005. Seeing spots: complex phase behavior in simple membranes. *Biochim. Biophys. Acta*. 1746:172–185.
7. Brown, D. A., and J. K. Rose. 1992. Sorting of GPI-anchored proteins to glycolipid-enriched membrane subdomains during transport to the apical cell-surface. *Cell*. 68:533–544.
8. Mouritsen, O. G., T. L. Andersen, A. Halperin, P. L. Hansen, A. F. Jakobsen, U. B. Jensen, M. O. Jensen, K. Jorgensen, T. Kaasgaard, C. Leidy, A. C. Simonsen, G. H. Peters, and M. Weiss. 2006. Activation of interfacial enzymes at membrane surfaces. *J. Phys. Cond. Mat.* 18:S1293–S1304.
9. Brown, W. J., K. Chambers, and A. Doody. 2003. Phospholipase A_2 (PLA_2) enzymes in membrane trafficking: mediators of membrane shape and function. *Traffic*. 4:214–221.
10. Kudo, I., and M. Murakami. 2002. Phospholipase A_2 enzymes. *Prostaglandins Other Lipid Mediat*. 68–69:3–58.
11. Balsinde, J., M. A. Balboa, P. A. Insel, and E. A. Dennis. 1999. Regulation and inhibition of phospholipase A_2. *Annu. Rev. Pharmacol. Toxicol.* 39:175–189.
12. Murakami, M., Y. Nakatani, G. Atsumi, K. Inoue, and I. Kudo. 1997. Regulatory functions of phospholipase A_2. *Crit. Rev. Immunol.* 17:225–283.

13. Dennis, E. A. 1973. Kinetic dependence of phospholipase A_2 activity on the detergent Triton X-100. *J. Lipid Res.* 14:152–159.

14. Zografi, G., R. Verger, and G. H. D. Haas. 1971. Kinetic analysis of the hydrolysis of lecithin monolayers by phospholipase A. *Chem. Phys. Lipids*. 7:185–206.

15. Verger, R., M. C. E. Mieras, and G. H. de Haas. 1973. Action of phospholipase A at interfaces. *J. Biol. Chem.* 248:4023–4034.

16. Verger, R., and G. H. D. Haas. 1973. Enzyme reactions in a membrane model 1: a new technique to study enzyme reactions in monolayers. *Chem. Phys. Lipids*. 10:127–136.

17. Bell, J. D., and R. L. Biltonen. 1989. Thermodynamic and kinetic studies of the interaction of vesicular dipalmitoylphosphatidylcholine with *Agkistrodon piscivorus piscivorus* phospholipase A_2. *J. Biol. Chem.* 264:225–230.

18. Bagatolli, L. A. 2006. To see or not to see: lateral organization of biological membranes and fluorescence microscopy. *Biochim. Biophys. Acta*. 1758:1541–1556.

19. Keller, D., N. B. Larsen, I. M. Moller, and O. G. Mouritsen. 2005. Decoupled phase transitions and grain-boundary melting in supported phospholipid bilayers. *Phys. Rev. Lett.* 94:025701.

20. Stottrup, B., S. Veatch, and S. Keller. 2004. Nonequilibrium behavior in supported lipid membranes containing cholesterol. *Biophys. J.* 86: 2942–2950.

21. Simonsen, A. C., and L. A. Bagatolli. 2004. Structure of spin-coated lipid films and domain formation in supported membranes formed by hydration. *Langmuir*. 20:9720–9728.

22. Simonsen, A. C., U. B. Jensen, and P. L. Hansen. 2006. Hydrolysis of fluid supported membrane islands by phospholipase A_2: time-lapse imaging and kinetic analysis. *J. Coll. Interf. Sci.* 301:107–115.

23. Jensen, M. H., E. J. Morris, and A. C. Simonsen. 2007. Domain shapes, coarsening and random patterns in ternary membranes. *Langmuir*. 23:8135–8141.

24. Grandbois, M., H. Clausen-Schaumann, and H. Gaub. 1998. Atomic force microscope imaging of phospholipid bilayer degradation by phospholipase A_2. *Biophys. J.* 74:2398–2404.

25. Kaasgaard, T., C. Leidy, J. H. Ipsen, O. G. Mouritsen, and K. Jorgensen. 2001. In situ atomic force microscope imaging of supported lipid bilayers. *Single Mol.* 2:105–108.

26. Nielsen, L. K., J. Risbo, T. H. Callisen, and T. Bjornholm. 1999. Lag-burst kinetics in phospholipase A_2 hydrolysis of DPPC bilayers visualized by atomic force microscopy. *Biochim. Biophys. Acta*. 1420:266–271.

27. Nielsen, L. K., K. Balashev, T. H. Callisen, and T. Bjornholm. 2002. Influence of product phase separation on phospholipase A_2 hydrolysis of supported phospholipid bilayers studied by force microscopy. *Biophys. J.* 83:2617–2624.

28. Balashev, K., M. Gudmand, L. Iversen, T. H. Callisen, A. Svendsen, and T. Bjornholm. 2003. *Humicola lanuginosa* lipase hydrolysis of mono-oleoyl-Rac-glycerol at the lipid-water interface observed by atomic force microscopy. *Biochim. Biophys. Acta*. 1615:93–102.

29. Balashev, K., N. J. Dinardo, T. H. Callisen, A. Svendsen, and T. Bjornholm. 2007. Atomic force microscope visualization of lipid bilayer degradation due to action of phospholipase A_2 and *Humicola lanuginosa* lipase. *Biochim. Biophys. Acta*. 1768:90–99.

30. Jensen, U. B., and A. C. Simonsen. 2005. Shape relaxations in a fluid supported membrane during hydrolysis by phospholipase A_2. *Biochim. Biophys. Acta. Rapid Rep.* 1715:1–5.

31. Op Den Kamp, J. A. F., J. De Gier, and L. L. M. van Deenen. 1974. Hydrolysis of phosphatidylcholine liposomes by pancreatic phospholipase A_2 at the transition temperature. *Biochim. Biophys. Acta.* 345:253–256.

32. Honger, T., K. Jorgensen, R. L. Biltonen, and O. G. Mouritsen. 1996. Systematic relationship between phospholipase A_2 activity and dynamic lipid bilayer microheterogeneity. *Biochemistry*. 35:9003–9006.

33. Sanchez, S. A., L. A. Bagatolli, E. Gratton, and T. L. Hazlett. 2002. A two-photon view of an enzyme at work: *Crotalus atrox* venom PLA_2 interaction with single-lipid and mixed-lipid giant unilamellar vesicles. *Biophys. J.* 82:2232–2243.

34. Leidy, C., O. G. Mouritsen, K. Jorgensen, and N. H. Peters. 2004. Evolution of a rippled membrane during phospholipase A_2 hydrolysis studied by time-resolved AFM. *Biophys. J.* 87:408–418.

35. Johnston, I., and L. J. Johnston. 2006. Ceramide promotes restructuring of model raft membranes. *Langmuir*. 22:11284–11289.

36. Chiantia, S., N. Kahya, J. Ries, and P. Schwille. 2006. Effects of ceramide on liquid-ordered domains investigated by simultaneous AFM and FCS. *Biophys. J.* 90:4500–4508.

37. Veatch, S. L., and S. L. Keller. 2005. Miscibility phase diagrams of giant vesicles containing sphingomyelin. *Phys. Rev. Lett.* 94:148101.

38. Veatch, S. L., K. Gawrisch, and S. L. Keller. 2006. Closed-loop miscibility gap and quantitative tie-lines in ternary membranes containing diphytanoyl pc. *Biophys. J.* 90:4428–4436.

39. Radhakrishnan, A., and H. McConnell. 2005. Condensed complexes in vesicles containing cholesterol and phospholipids. *Proc. Natl. Acad. Sci. USA*. 102:12662–12666.

40. Ipsen, J., G. Karlström, O. Mouritsen, H. Wennerström, and M. Zuckermann. 1987. Phase-equilibria in the phosphatidylcholine-cholesterol system. *Biochim. Biophys. Acta*. 905:162–172.

41. Elliott, R., K. Katsov, M. Schick, and I. Szleifer. 2005. Phase separation of saturated and mono-unsaturated lipids as determined from a microscopic model. *J. Chem. Phys.* 122:044904.

42. Leidy, C., L. Linderoth, T. L. Andresen, O. G. Mouritsen, K. Jorgensen, and G. H. Peters. 2006. Domain-induced activation of human phospholipase A_2 type IIA: local versus global lipid composition. *Biophys. J.* 90:3165–3175.

43. Filippov, A., G. Oradd, and G. Lindblom. 2003. The effect of cholesterol on the lateral diffusion of phospholipids in oriented bilayers. *Biophys. J.* 84:3079–3086.

44. Radhakrishnan, A., and H. M. McConnell. 1999. Condensed complexes of cholesterol and phospholipids. *Biophys. J.* 77:1507–1517.

45. McConnell, H. M., and A. Radhakrishnan. 2003. Condensed complexes of cholesterol and phospholipids. *Biochim. Biophys. Acta.* 1610:159–173.

46. Smondyrev, A. M., and M. L. Berkowitz. 1999. Structure of dipalmitoylphosphatidylcholine/cholesterol bilayer at low and high cholesterol concentrations: molecular dynamics simulation. *Biophys. J.* 77:2075–2089.

47. Peters, G. H., M. S. Moller, K. Jorgensen, P. Ronnholm, M. Mikkelsen, and T. L. Andresen. 2007. Secretory phospholipase A_2 hydrolysis of phospholipid analogues is dependent on water accessibility to the active site. *J. Am. Chem. Soc.* 129:5451–5461.

48. Andresen, T. L., and K. Jorgensen. 2005. Synthesis and membrane behavior of a new class of unnatural phospholipid analogs useful as phospholipase A_2 degradable liposomal drug carriers. *Biochim. Biophys. Acta*. 1669:1–7.

49. de la Serna, J., J. Perez-Gil, A. C. Simonsen, and L. A. Bagatolli. 2004. Cholesterol rules—direct observation of the coexistence of two fluid phases in native pulmonary surfactant membranes at physiological temperatures. *J. Biol. Chem.* 279:40715–40722.

50. Lusis, A. J. 2000. Atherosclerosis. *Nature*. 407:233–241.

51. Ivandic, B., L. W. Castellani, X. P. Wang, J. H. Qiao, M. Mehrabian, M. Navab, A. M. Fogelman, D. S. Grass, M. E. Swanson, M. C. de Beer, F. de Beer, and A. J. Lusis. 1999. Role of group II secretory phospholipase A_2 in atherosclerosis. 1. Increased atherogenesis and altered lipoproteins in transgenic mice expressing group IIa phospholipase A_2. *Arterioscler. Thromb. Vasc. Biol.* 19:1284–1290.

52. Veatch, S. L., O. Soubias, S. L. Keller, and K. Gawrisch. 2007. Critical fluctuations in domain-forming lipid mixtures. *Proc. Nat. Acad. Sci. USA*. 104:17650–17655.

53. de Almeida, R. F. M., J. Borst, A. Fedorov, M. Prieto, and A. J. W. G. Visser. 2007. Complexity of lipid domains and rafts in giant unilamellar vesicles revealed by combining imaging and microscopic and macroscopic time-resolved fluorescence. *Biophys. J.* 93:539–553.